

Published in final edited form as:

J Immunol. 2018 December 01; 201(11): 3373–3382. doi:10.4049/jimmunol.1700614.

ABIN2 Function Is Required To Suppress DSS-Induced Colitis by a Tpl2-Independent Mechanism

Sambit K. Nanda^{*,1}, Tsunehisa Nagamori^{*,1,2}, Mark Windheim^{*,3}, Sylvia Amu^{†,4}, Gabriella Aviello^{†,5}, Janet Patterson-Kane^{‡,6}, J. Simon C. Arthur[§], Steven C. Ley[¶], Padraic Fallon[†], and Philip Cohen^{*}

^{*}Medical Research Council Protein Phosphorylation and Ubiquitylation Unit, University of Dundee, Dundee DD1 5EH, United Kingdom [†]Trinity Biomedical Sciences Institute, School of Medicine, Trinity College Dublin, Dublin 2, Ireland [‡]School of Veterinary Medicine, University of Glasgow, Glasgow G61 1QH, United Kingdom [§]Division of Cell Signalling and Immunology, School of Life Sciences, University of Dundee, Dundee DD1 5EH, United Kingdom [¶]The Francis Crick Institute, London NW1 1AT, United Kingdom

Abstract

The A20-binding inhibitor of NF- κ B 2 (ABIN2) interacts with Met1-linked ubiquitin chains and is an integral component of the tumor progression locus 2 (Tpl2) kinase complex. We generated a knock-in mouse expressing the ubiquitin-binding-defective mutant ABIN2[D310N]. The expression of Tpl2 and its activation by TLR agonists in macrophages or by IL-1 β in fibroblasts from these mice was unimpaired, indicating that the interaction of ABIN2 with ubiquitin oligomers is not required for the stability or activation of Tpl2. The ABIN2[D310N] mice displayed intestinal inflammation and hypersensitivity to dextran sodium sulfate-induced colitis, an effect that was mediated by radiation-resistant cells rather than by hematopoietic cells. The IL-1 β -dependent induction of cyclooxygenase 2 (COX2) and the secretion of PGE₂ was reduced in mouse embryonic fibroblasts and intestinal myofibroblasts (IMFs) from ABIN2[D310N] mice. These observations are similar to those reported for the Tpl2 knockout (KO) mice (Roulis et al. 2014. *Proc. Natl. Acad. Sci. USA* 111: E4658–E4667), but the IL-1 β -dependent production of COX2 and PGE₂ in mouse embryonic fibroblasts or IMFs was unaffected by pharmacological inhibition of Tpl2 in wild-type mice. The expression of ABIN2 is decreased drastically in Tpl2 KO mice. These and other lines of evidence suggest that the hypersensitivity of Tpl2 KO mice to dextran sodium sulfate-induced colitis is not caused by the loss of Tpl2 catalytic activity but by

Address correspondence and reprint requests to Prof. Philip Cohen, University of Dundee, Sir James Black Centre, Dow Street, Dundee DD1 5EH, U.K. p.cohen@dundee.ac.uk.

¹S.K.N. and T.N. are joint first authors.

²Current address: Department of Pediatrics, Asahikawa Medical University, Asahikawa, Hokkaido, Japan.

³Current address: Institute of Biochemistry, Hannover Medical School, Hannover, Germany.

⁴Current address: University College Cork, Cork, Ireland.

⁵Current address: Aberdeen University, Aberdeen, U.K.

⁶Current address: Flagship Biosciences Inc., Denver, CO.

Disclosures

The authors have no financial conflicts of interest.

ORCIDs: 0000-0002-9094-1263 (J.P.-K.); 0000-0002-8401-7293 (P.F.).

the loss of ABIN2, which impairs COX2 and PGE₂ production in IMFs by a Tpl2 kinase-independent pathway.

The protein kinase tumor progression locus 2 (Tpl2, also called MAP3K8) forms a complex with two other proteins, termed NF- κ B1 (also called p105) (1) and the A20-binding inhibitor of NF- κ B 2 (ABIN2). The Tpl2 complex is activated by many inflammatory stimuli, including TNF, IL-1, and ligands that activate pattern recognition receptors (2). Tpl2 activation is mediated by the IKK β -catalyzed phosphorylation of both NF- κ B1 (3) and the Tpl2 catalytic subunit itself (4). This induces the dissociation of Tpl2 from the other subunits and its interaction with 14-3-3 proteins (5).

The molecular functions of Tpl2 include activation of the protein kinases MEK1 and MEK2, which switch on the MAPKs ERK1 and ERK2 (6), and activation of MAPK kinases 3 and 6, which switch on p38 α MAPK (7, 8). However, Tpl2 is only rate limiting for the activation of p38 α MAPK by some stimuli (7) because p38 α MAPK can also be activated by MKK4, depending on the agonist or cell type. Tpl2 has many important roles in the innate immune system. For example, it is required for the processing of pre-TNF- α to TNF- α (9) for LPS-induced septic shock (6) and for effective immune responses to infection by *Listeria monocytogenes* and *Mycobacterium tuberculosis* (10).

Tpl2 is also reported to have important roles in inflammatory bowel diseases (IBD). TNF- α -induced Crohn-like IBD was attenuated in Tpl2 knockout (KO) mice (11), and a small molecule Tpl2 inhibitor protected mice against dextran sodium sulfate (DSS)-induced colitis (8), indicating that Tpl2 catalytic activity is required for colitis in this model. Consistent with these findings, genome-wide association studies identified a single nucleotide polymorphism in *MAP3K8*, the gene encoding Tpl2, which pre-disposes to IBD in humans (12), and monocyte-derived macrophages homozygous for this single nucleotide polymorphism expressed higher levels of Tpl2 mRNA and protein and secreted higher levels of TNF- α and other cytokines when stimulated with ligands that activate different pattern recognition receptors (13).

In contrast to the above-mentioned studies, Tpl2 KO mice were reported to be hypersensitive to DSS-induced colitis (14). This effect was mediated by intestinal myofibroblasts (IMFs) because mice with an IMF-specific ablation of Tpl2 were similarly susceptible to DSS-induced colitis. Tpl2 KO mice displayed the same impaired compensatory proliferation in crypts and extensive ulcerations without a significant change in the inflammatory response being observed. The induction of cyclooxygenase 2 (COX2) was reduced in IMFs from Tpl2 KO mice, and the consequent reduction in PGE₂ secretion appeared to underlie the defect because the administration of PGE₂ rescued the Tpl2 KO mice from defects in crypt function and susceptibility to colitis (14).

Each subunit of the Tpl2 complex is essential for the stability of the others. Consequently, the KO of NF- κ B1 is accompanied by greatly reduced expression of Tpl2 and ABIN2 (15, 16), whereas Tpl2 expression is greatly reduced in ABIN2 KO cells (1, 17). The KO of the Tpl2 catalytic subunit also leads to a drastic reduction in ABIN2 expression (18). For these reasons it has been impossible to determine whether ABIN2 has any physiological roles that

are independent of Tpl2. In this study, we show that the IL-1 β -dependent production of COX2 and PGE₂ in fibroblasts is an ABIN2-dependent process that is independent of Tpl2 catalytic activity and suggests that the hypersensitivity of Tpl2 KO mice to DSS-induced colitis is explained by the loss of ABIN2 in IMFs and not by the lack of Tpl2 catalytic activity.

Materials and Methods

Materials

Pam₃CSK₄ was from Invivogen, and LPS (*Escherichia coli* O55:B5) was from Alexis Biochemicals. Abs that recognize ERK1/ERK2 phosphorylated at their Thr-Glu-Tyr motifs (197G2; 4377), Abs that recognize all forms of ERK1/ERK2 (137F5; 4695), and Abs recognizing GAPDH (14C10; 2118) and cyclooxygenase 1 (COX1) were from Cell Signaling Technology. An Ab-recognizing NF- κ B1 was from Abcam (E381; ab32360), a COX2 Ab was from Cayman Chemical (160106), and an anti-Tpl2 Ab was from Santa Cruz Biotechnology (M-20; SC-720).

A rabbit polyclonal ABIN2 Ab for immunoblotting and a NF- κ B1 Ab for immunoprecipitation have been described previously (1). An Ab that immunoprecipitates Tpl2 was raised in sheep against amino acid residues 398–417 of mouse Tpl2 (CQSLDSALFERKRLLSRKELE) by the Ab production team of the Medical Research Council Protein Phosphorylation and Ubiquitylation Unit coordinated by Dr. J. Hastie. The Ab was affinity purified on agarose beads to which the Ag had been coupled covalently (Sheep 688A) and can be ordered from the reagents section of the Medical Research Council Protein Phosphorylation and Ubiquitylation Unit web site (<https://mrcppureagents.dundee.ac.uk/>). Ab produced from the second bleed was used for the experiments reported in this paper. The PGE₂ ELISA Kit (514010; Cayman Chemical) was used to quantitate PGE₂ and was used according to the manufacturer's instructions. Secondary Abs conjugated to HRP were from Pierce.

Immunoprecipitation of Tpl2 and NF- κ B1 from cell extracts

For immunoprecipitation, 0.5 mg of cell extract protein was incubated for 2 h with 5 μ g of anti-Tpl2. Protein G–Sepharose beads (25 μ l) were added and incubated by end-over-end rotation for 30 min at 4°C. Immunoprecipitation of NF- κ B1 was carried out as described (19). Cell extract protein (0.5 mg protein) was incubated for 4 h with 14 μ g of anti-NF- κ B1 coupled covalently to 40 μ l of protein G–Sepharose beads. The beads were collected by centrifugation, washed three times with cell lysis buffer, denatured in SDS, subjected to SDS-PAGE, and immunoblotted.

Quantitative RT-PCR analysis

Total RNA was extracted from cultured cells using E.Z.N.A. MicroElute Total RNA Kit (R6831-01; VWR International), and cDNA was generated using iScript transcriptase (1708890; Bio-Rad Laboratories). Quantitative PCR was performed using SsoFast EvaGreen Supermix (172-5200; Bio-Rad Laboratories). Primer sets for *COX2* and *COX1* were as follows: *COX2* forward 5'-CCAGCACTTCACCCATCAGTT-3', *COX2* reverse 5'-

ACCCAGGTCCTCGCTTATGA-3'; *COX1* forward 5'-
AAGGCAGAGGCAGTTGGATCT-3', *COX1* reverse 5'-CATGGCTGG
CCTAGAACTCACT-3'.

Cell culture and transfection

Human embryonic kidney 293 cells overexpressing the IL-1 receptor (IL-1R cells) were a kind gift from Dr. X. Li (Cleveland Clinic Foundation). The cells were cultured at 37°C with DMEM containing 10% (v/v) FBS, 1 mM sodium pyruvate, antibiotics (100 U/ml penicillin and 100 µg/ml streptomycin), and glutamax at a concentration recommended by the manufacturer (Life Technologies). Human embryonic kidney 293 cells were transiently transfected with 1 µg of DNA/ml of cell culture medium using polyethylenimine (Sigma-Aldrich) as described (20). The cells were harvested 36 h posttransfection and lysed with ice-cold lysis buffer. Primary bone marrow-derived macrophages (BMDM) (21) and primary mouse embryonic fibroblasts (MEFs) (22) were generated as described previously. Colonic myofibroblast isolation was performed as described previously (14) with minor modifications. Briefly, colons from 7- to 9-d-old pups were dissected, and the colon was washed with PBS containing antibiotics after opening it longitudinally. It was then cut into 2- to 3-mm pieces and incubated for 1 h at 37°C with DMEM containing 75 U/ml Collagenase XI (Sigma-Aldrich) and 0.1 mg/ml Dispase (Roche). After low speed centrifugation, the pellet was washed four times with 2% (w/v) sorbitol in DMEM and cultured in 12-well plates. The cells were passaged five times and used in further experiments after confirming that >95% were positive for CD90.2 (BioLegend).

Generation of ABIN2[D310N] knock-in and ABIN2 KO mice

ABIN2 is encoded by the *TNIP2* gene, which comprises six main exons. To generate the Asp310Asn knock-in mutation, a targeting vector was constructed to make the desired change in exon 5 of the *TNIP2* gene. In addition, LoxP sites were introduced upstream of exon 4 and downstream of exon 6. To allow for selection, a neomycin resistance gene incorporating a poly A trap using the splice donor sequence from exon 2 of *TNIP2* was incorporated and flanked by Frt sites. The fragments for the arms of homology were cloned from an appropriate bacterial artificial chromosome clone using the PCR and were sequenced to confirm that there were no PCR-introduced mutations. The primer sequences used to clone these fragments are listed in Supplemental Table I, and the complete sequence of the targeting vector is available on request. Targeting was carried out in E14 embryonic stem cells as described previously (23). Following selection, colonies were screened by RT-PCR to detect mRNA corresponding to the neomycin cassette spliced onto the final exon of *TNIP2*. Correct incorporation of the vector in positive colonies was further confirmed by genomic PCR. Positive embryonic stem cell clones were injected into blastocysts, and the resulting chimeric mice were crossed to Frt transgenic mice. This allowed the removal of the neomycin cassette when germline transmission of the knock-in allele occurred. The Asp310Asn allele was bred away from the Flp transgene, and the mice were further backcrossed to C57BL/6J mice for a minimum of 10 generations. To generate ABIN2 KO mice, the ABIN2[D310N] knock-in mice were crossed to a Cre transgenic line able to delete in the germline. Routine genotyping of both the ABIN2[D310N] and ABIN2 KO alleles was

carried out by PCR on genomic DNA from ear biopsy specimens. Primer sequences for genotyping are shown in Supplemental Table II.

Animals were maintained under specific pathogen-free conditions consistent with European Union and U.K. regulations. Mice were housed in individually ventilated cages and provided with free access to food and water. The work was performed under a U.K. Home Office project license awarded after recommendation by the University of Dundee Ethical Review Committee or in compliance with the Health Products Regulatory Authority of Ireland and approved by Trinity College Dublin's Bio-Resources Unit ethical review board.

DSS-induced colitis

DSS-induced colitis was carried out with mice kept in the animal facility of Trinity College Biomedical Sciences Institute. Colitis was induced by feeding mice every second day with 2.5% (w/v) DSS (molecular mass 35–50 kDa) from ICN Biochemical dissolved in tap water. Mice were given DSS in tap water for 5 d followed by tap water without DSS until the end of the experiment on day 9–10. The induction of colitis was determined by measuring a disease activity index (DAI). The DAI was calculated for individual mice on each day based on weight loss, occult blood, and stool consistency. A score was given for each parameter, with the sum of the scores used as the DAI (Supplemental Table III). Blood in feces was detected using a HEMDETECT occult blood detection kit (Dipro Diagnostic Products). At autopsy, colon lengths and cecum weight were recorded, and the colon was processed for histology and cytokine quantification.

Bone marrow chimeras

Bone marrow transfers were carried out to create chimeric mice to determine whether the presence of the ABIN2[D310N] mutant in the radio-resistant cells and/or radio-sensitive hematopoietic cells caused the colitis phenotype. Bone marrow was collected from the femur and tibia of congenic wild-type (WT) mice (expressing the CD45.1 leukocyte Ag) or ABIN2[D310N] mice (expressing the CD45.2 leukocyte Ag) by flushing with PBS. RBCs were lysed in RBC lysis buffer (Sigma-Aldrich). After several washing steps, cells were resuspended in PBS at 1×10^8 cells/ml, and 0.1 ml of this cell suspension was injected retro-orbitally into lethally irradiated (10 Gy) donor mice. Four chimera groups were generated: WT > WT (WT cells expressing CD45.1 into WT mice expressing CD45.2), WT > ABIN2[D310N] (WT cells expressing CD45.1 into ABIN2[D310N] mice expressing CD45.2), ABIN2[D310N] > WT (ABIN2[D310N] cells expressing CD45.2 into WT mice expressing CD45.1), and ABIN2[D310N] > ABIN2[D310N] (ABIN2[D310N] cells expressing CD45.2 into ABIN2[D310N] mice expressing CD45.2). The use of CD45.1-expressing congenic mice facilitated verification of proper reconstitution in the chimeric mice. Eight weeks after bone marrow transfer, mice were subjected to the DSS-induced colitis experiment described above.

Histopathological analysis

The colons of mice kept in the animal facilities of the School of Life Sciences at Dundee and the Trinity Biomedical Sciences Institute in Dublin were used for these experiments. The colon of each mouse was removed, and 1 cm of the distal colon was fixed in 10% neutral

buffered formalin and embedded in paraffin. Tissue sections were stained with H&E. The histology of both the colon and tissue sections was assessed and scored by a veterinary pathologist (J.P.-K.), blinded to the genotype of the mice in the different cohorts. The scores were generated as a combination of inflammatory cell infiltration (score 0–3) and tissue damage (score 0–3). The presence of occasional inflammatory cells in the lamina propria was scored as 0, increased numbers of inflammatory cells in the lamina propria was assigned score 1, confluence of inflammatory cells extending into the submucosa was scored as 2, and transmural extension of the infiltrate was scored as 3. For tissue damage, no mucosal damage was scored as 0, lympho-epithelial lesions were scored as 1, surface mucosal erosion or focal ulceration was scored as 2, and extensive mucosal damage and extension into deeper structures of the bowel wall were scored as 3. The combined histological score ranged from 0 (no changes) to 6 (extensive infiltration and tissue damage).

Reproducibility and statistical analysis

The experiments reported in this paper were repeated at least three times with similar results unless stated otherwise. Statistical analyses were performed with GraphPad Prism Software, and quantitative data in graphs and bar charts are presented as the arithmetic mean \pm SEM. Statistical analyses were performed using either a Student *t* test or a Mann–Whitney *U* test with differences in DAI in chimera DSS studies determined by ANOVA and Tukey multiple comparison tests of area under curve data from individual mice.

Results

Generation of ABIN2[D310N] knock-in mice

We previously generated knock-in mice, in which ABIN1 was replaced by the ubiquitin-binding-defective ABIN1[D485N] mutant (24). In this study, we generated the equivalent ABIN2[D310N] mutant of the related mouse ABIN2 protein (25) (Fig. 1A, 1B) after checking that the equivalent human mutant (ABIN2[D309N]) was unable to capture ubiquitin chains or the ubiquitylated forms of IL receptor-associated kinase 1 (IRAK1) from the cell extracts (Fig. 1C). The ubiquitin chains attached to IRAK1 include Met1-linked ubiquitin linkages (26), which are captured preferentially by ABIN2 (27, 28).

The ABIN2[D310N] mice were born at near-normal Mendelian frequencies (19% of 329 mice analyzed) and were of a similar size and weight to WT mice. The endogenous ABIN2[D310N] protein was expressed at lower levels than WT ABIN2 in primary BMDM (Fig. 2A), and quantitation of the results from three different preparations of WT BMDM and ABIN2[D310N] BMDM indicated that expression was reduced by 66%. The expression of ABIN2[D310N] was also lower than WT ABIN2 in IMFs (Fig. 2B) but was expressed at similar levels to WT ABIN2 in MEFs (Fig. 2C). The reduced expression of ABIN2[D310N] in BMDM is likely to be caused by an increased rate of degradation because incubation with the proteasome inhibitor MG132 normalized the level of expression of ABIN2[D310N] to that observed in WT BMDM (Fig. 2D).

Despite the reduced expression of the ABIN2[D310N] mutant in BMDM and IMFs, the two variants of the Tpl2 catalytic subunit, Tpl2_L and Tpl2_S (15), and NF- κ B1 were expressed at

similar levels to those observed in cells expressing WT ABIN2 (Fig. 2A, 2B). In contrast, Tpl2 expression in BMDM from ABIN2 KO mice, which were generated by crossing ABIN2[D310N] mice to Ball1 Cre (see Materials and Methods), was reduced drastically (Fig. 2A), as reported in earlier studies with ABIN2 KO cells (17, 18).

Importantly, and despite the reduced expression of the ABIN2[D310N] mutant in BMDM, similar amounts of the mutant ABIN2[D310N] and WT ABIN2 were immunoprecipitated with anti-Tpl2 (Fig. 2E) or anti-p105/NF- κ B1 (Fig. 2F), indicating that the ABIN2[D310N] associated with the Tpl2 complex is more stable than the ABIN2[D310N] not bound to Tpl2. These observations may also explain why Tpl2 is expressed at similar levels in ABIN2[D310N] and WT cells.

Consistent with the similar expression of Tpl2 in cells from ABIN2[D310N] and WT mice, the acute activation of ERK1 and ERK2 induced by the TLR4 agonist LPS (Fig. 3A) or the TLR1/2 agonist Pam3CSK4 (Fig. 3B) was similar in BMDM from the mutant and WT mice. The acute activation of ERK1/2 induced by IL-1 β was also similar in MEFs from ABIN2[D310N] and WT mice (Fig. 3C). The early activation of ERK1/2 in BMDM (Fig. 3D) or MEFs (Fig. 3E) was catalyzed by Tpl2 because it was prevented by Compound 34 (C34), a potent and relatively specific Tpl2 inhibitor (29). Thus, ubiquitin binding to ABIN2 is not required for the activation of Tpl2.

The ABIN2[D310N] mice are hypersensitive to DSS-induced colitis

The ABIN1[D485N] mice develop an enlarged spleen and enlarged lymph nodes by 3 mo of age, produce Abs to their own DNA and nuclear Ags after 4–5 mo, and develop severe inflammation of the kidneys, liver, and lungs by 6 mo. The ABIN2[D310N] mice did not display any of these phenotypes. However, pathological examination of the ABIN2[D310N] mice at the University of Dundee revealed increased infiltration of the lamina propria of the small intestine with large numbers of myeloid cells after 6 mo of age (Fig. 4A) but not after 2–3 mo. In contrast, 2-mo-old mice transported from the University of Dundee to Trinity College Dublin displayed intestinal inflammation when they were 3–4 mo old. In contrast, the ABIN2[D310N] mice kept in London did not display intestinal inflammation at 6 mo of age. This variability may reflect the different bacterial populations in the gut of the animals at each location. Nevertheless, the infiltration of intestinal cells with myeloid cells is characteristic of human patients with IBD and suggested that the mice might be more susceptible to colitis. We, therefore, studied the effect of oral administration of DSS, which is toxic to the colonic epithelium (30) and triggers inflammation by disrupting the compartmentalization of commensal bacteria in the gut (31).

We assessed the effect of DSS administration in ABIN2[D310N] mice compared with age- and sex-matched WT littermate control animals. These studies were performed at Trinity College Dublin when the mice were 3–4 mo old. From day 7 of DSS treatment, there was a significantly ($p < 0.05$) greater loss in body weight of the ABIN2[D310N] mice relative to WT control mice (Fig. 4B). The cumulative DAI scores demonstrated colitis was more severe in the ABIN2[D310N] mice from days 8 and 9 ($p < 0.0005$ – 0.0001) compared with WT animals, (Fig. 4C), with marked rectal bleeding in ABIN2[D310N] mice compared with WT mice (Fig. 4D).

The evaluation of colon length is the parameter that shows the lowest mouse-to-mouse variability in the model of DSS-induced colitis (32). To further assess the severity of colitis, colon length was, therefore, measured in DSS-fed WT and ABIN2[D310N] mice. Colons of the ABIN2[D310N] mice were significantly ($p < 0.01$) shorter, on average 20% shorter, than those of the WT mice treated with DSS, consistent with the more severe inflammation of the colon in the knock-in mice (Fig. 4E).

The clinical assessments described in the preceding paragraphs were validated by histological examination of representative colon sections (Fig. 4F). In agreement with previous studies (31), we observed marked histopathological changes in H&E-stained colons of DSS-treated WT mice, characterized by crypt loss and infiltrating leukocytes. However, there was only minimal evidence of necrosis and ulceration in the colons of WT mice. In contrast, colonic sections of DSS-fed ABIN2[D310N] mice displayed severe transmural inflammation with focal areas of extensive ulceration and necrotic lesions. Inflammatory infiltrates filled the lamina propria and submucosa in areas where the mucosa was intact and often effaced the normal architecture of the tissue. Submucosal edema was often marked in areas of ulceration (Fig. 4F). The colons of DSS-treated ABIN2[D310N] mice had significantly elevated levels of myeloperoxidase activity consistent with marked myeloid cell infiltration (Fig. 4G). These data indicate that ABIN2[D310N] mice are more susceptible to DSS-induced colitis with delayed recovery from intestinal injury.

Involvement of radiation-resistant cells in colitis in ABIN2[D310N] mice

To determine the cell populations involved in DSS-induced colitis in ABIN2[D310N] mice, we generated four groups of bone marrow chimeras. Following lethal irradiation of the WT and ABIN2[D310N] mice (to destroy the hematopoietic cells), bone marrow from either WT or ABIN2[D310N] knock-in mice was transplanted into the irradiated mice. The hematopoietic cells were allowed to regenerate from the injected bone marrow cells for 6 wk, and bone marrow reconstitution was verified after 6 wk by staining for CD45.1 and CD45.2 in blood cells. The mice were then treated with DSS. We found that the DAI in the ABIN2[D310N] mice was similar whether they had received WT bone marrow or bone marrow from the ABIN2[D310N] mice. Similarly, the DAI in the WT mice was similar whether they had received WT bone marrow or bone marrow from the ABIN2[D310N] mice. However, the DAI was consistently less severe in the recipient WT mice than the recipient ABIN2[D310N] mice ($p < 0.05$), irrespective of whether they had received bone marrow from the WT or ABIN2[D310N] mice (Fig. 5A). Consistent with the above data, the colon length was ~20% shorter in the ABIN2[D310N] recipient chimeric mice than in the WT recipient mice (Fig. 5B). Taken together, these results indicate that radiation-resistant cells in the gut have an important role in driving colitis in ABIN2[D310N] mice.

Reduced IL-1–dependent expression of COX2 and secretion of PGE₂ in MEFs and IMFs of ABIN2[D310N] mice

The hypersensitivity of ABIN2[D310N] mice to DSS-induced colitis by a mechanism involving the radiation-resistant cells was similar to observations made with Tpl2 KO mice (14). Because the expression of ABIN2 is greatly reduced in Tpl2 KO mice (18), we

wondered whether the phenotype of the Tpl2 KO mice might be caused by the loss of ABIN2 expression rather than the loss of Tpl2 catalytic activity.

The hypersensitivity of Tpl2 KO mice to DSS-induced colitis is caused by reduced secretion of PGE₂, resulting from reduced IL-1 β -dependent expression of COX2 in IMFs (14). We, therefore, compared the production of these molecules in fibroblasts from ABIN2[D310N] and WT mice. The IL-1 β -dependent induction of *COX2* mRNA was reduced in ABIN2[D310N] MEFs compared with WT MEFs (Fig. 6A), but *COX1* mRNA levels were unchanged (Fig. 6B). Consistent with these findings, the IL-1 β -dependent induction of COX2 protein was reduced in MEFs and IMFs from ABIN2[D310N] mice (Fig. 6C, 6D) and, consequently, the secretion of PGE₂ was also decreased markedly (Fig. 6E, 6F). Because the level of expression of the ABIN2[D310N] is similar to WT ABIN2 in MEFs (Fig. 2C), these results indicate that ubiquitin binding to ABIN2 is required for robust IL-1 β -dependent production of COX2 and PGE₂ secretion in MEFs.

Although the Tpl2 inhibitor C34 suppressed the rapid initial activation of ERK1/2 observed after stimulating MEFs with IL-1 β for 15 min, it did not suppress the activation of ERK1 and ERK2 observed after stimulation for 3–6 h (Fig. 6G), indicating that Tpl2 activity was not rate limiting for ERK1/2 activation at these later times. Consistent with these results, the IL-1 β -stimulated production of COX2 and secretion of PGE₂, which occurred between 3 and 6 h after stimulation with IL-1 β , was also unaffected by C34 in either MEFs or IMFs (Fig. 6H, 6I). Thus, the decreased induction of COX2 and PGE₂ secretion in ABIN2[D310N] mice is independent of Tpl2 catalytic activity.

The LPS-stimulated production of COX2 is Tpl2-dependent in BMDM

In contrast to MEFs, it has been reported that the LPS-stimulated production of COX2 in BMDM is mediated by Tpl2 catalytic activity (33). Consistent with these reports, we confirmed that C34 suppressed both LPS-induced *COX2* mRNA (Supplemental Fig. 1A) and protein (Supplemental Fig. 1B). However, similar to IL-1 β stimulation in MEFs (Fig. 6G), C34 suppressed the initial activation of ERK1/2 observed after 15 min but not the lower level of ERK1/2 activation observed between 3 and 6 h after stimulation with LPS (Supplemental Fig. 1B). A MAP3K family member distinct from Tpl2 is, therefore, rate limiting for ERK1/2 activation after prolonged stimulation of BMDM with LPS or fibroblasts with IL-1 β .

Discussion

In this study, we show that mice expressing an ABIN2 mutant that cannot interact with ubiquitin chains are more susceptible to intestinal inflammation and hypersensitive to DSS-induced colitis (Fig. 4). These mice express normal levels of Tpl2, and the activation of Tpl2 by IL-1 β and ligands that activate TLRs is unimpaired in either fibroblasts or BMDM (Fig. 3). These results indicate that ubiquitin binding to ABIN2 is not required for either the activation or stability of Tpl2.

Interestingly, the hypersensitivity of ABIN2[D310N] mice to DSS-induced colitis (Fig. 4) was strikingly similar to previous studies in Tpl2 KO mice (14). In both cases,

hypersensitivity was caused by the radiation-resistant cells and not by hematopoietic cells (Fig. 5) and could be explained by reduced induction of COX2 and secretion of PGE₂ in IMFs (14) (Fig. 6). The expression of ABIN2 is greatly reduced in Tpl2 KO mice, and two lines of evidence suggest that it is the decrease in ABIN2 expression and not the loss of Tpl2 catalytic activity that underlies the reduced production of COX2 and PGE₂ in Tpl2 KO MEFs and, hence, hypersensitivity to colitis. First, the IL-1 β -dependent production of COX2 or PGE₂ in fibroblasts is unaffected by pharmacological inhibition of Tpl2 (Fig. 6). Second, DSS-induced colitis is actually suppressed by a small-molecule inhibitor of Tpl2 (8). Thus, ABIN2 controls COX2 and PGE₂ production and protects against DSS-induced colitis by a Tpl2-independent mechanism. In contrast, the inhibition of Tpl2 catalytic activity appears to protect mice against IBD by suppressing the inflammatory actions of TNF (8). Elucidating the mechanism by which ubiquitin binding to ABIN2 stimulates the IL-1 β -dependent production of COX2 in fibroblasts will be an interesting topic for future research. The activation of Tpl2 is known to induce its dissociation from ABIN2, and our working hypothesis is that, when released from the Tpl2 catalytic subunit, ubiquitin chain-associated ABIN2 interacts with another protein to stimulate COX2 production. This might be another protein kinase because the interaction of ABIN2 with other protein kinases, such as LKB1 (34), IKK α (35), and TIE2 (36) has been reported.

Interestingly, reduced expression of Tpl2 has been reported in IMFs isolated from the inflamed ileum of IBD patients (14). Clearly, it will now be important to examine whether variation in *TNIP2*, the gene encoding ABIN2, underlies or predisposes to IBD in human populations.

Supplementary Material

Refer to Web version on PubMed Central for supplementary material.

Acknowledgments

This work was supported by the U.K. Medical Research Council (Grant MRC_MR/K000985/1), Boehringer-Ingelheim, GlaxoSmithKline, and Merck Serono. T.N. was funded by the Uehara Memorial Foundation for International Students (Grant 201440246). S.C.L. is supported by core funding from The Francis Crick Institute.

Abbreviations used in this article

ABIN2	A20-binding inhibitor of NF- κ B 2
BMDM	bone marrow-derived macrophage
C34	Compound 34
COX1	cyclooxygenase 1
COX2	cyclooxygenase 2
DAI	disease activity index
DSS	dextran sodium sulfate

IBD	inflammatory bowel disease
IMF	intestinal myofibroblast
IRAK1	IL receptor-associated kinase 1
KO	knockout
MEF	mouse embryonic fibroblast
Tpl2	tumor progression locus 2
WT	wild-type

References

- Lang V, Symons A, Watton SJ, Janzen J, Soneji Y, Beinke S, Howell S, Ley SC. ABIN-2 forms a ternary complex with TPL-2 and NF-kappa B1 p105 and is essential for TPL-2 protein stability. *Mol Cell Biol.* 2004; 24:5235–5248. [PubMed: 15169888]
- Arthur JS, Ley SC. Mitogen-activated protein kinases in innate immunity. *Nat Rev Immunol.* 2013; 13:679–692. [PubMed: 23954936]
- Waterfield M, Jin W, Reiley W, Zhang M, Sun SC. IkappaB kinase is an essential component of the Tpl2 signaling pathway. *Mol Cell Biol.* 2004; 24:6040–6048. [PubMed: 15199157]
- Cho J, Tschlis PN. Phosphorylation at Thr-290 regulates Tpl2 binding to NF-kappaB1/p105 and Tpl2 activation and degradation by lipopolysaccharide. *Proc Natl Acad Sci USA.* 2005; 102:2350–2355. [PubMed: 15699325]
- Ben-Addi A, Mambole-Dema A, Brender C, Martin SR, Janzen J, Kjaer S, Smerdon SJ, Ley SC. IκB kinase-induced interaction of TPL-2 kinase with 14-3-3 is essential for Toll-like receptor activation of ERK-1 and -2 MAP kinases. *Proc Natl Acad Sci USA.* 2014; 111:E2394–E2403. [PubMed: 24912162]
- Dumitru CD, Ceci JD, Tsatsanis C, Kontoyiannis D, Stamatakis K, Lin JH, Patriotis C, Jenkins NA, Copeland NG, Kollias G, Tschlis PN. TNF-alpha induction by LPS is regulated posttranscriptionally via a Tpl2/ERK-dependent pathway. *Cell.* 2000; 103:1071–1083. [PubMed: 11163183]
- Pattison MJ, Mitchell O, Flynn HR, Chen CS, Yang HT, Ben-Addi H, Boeing S, Snijders AP, Ley SC. TLR and TNF-R1 activation of the MKK3/MKK6-p38α axis in macrophages is mediated by TPL-2 kinase. *Biochem J.* 2016; 473:2845–2861. [PubMed: 27402796]
- Senger K, Pham VC, Varfolomeev E, Hackney JA, Corzo CA, Collier J, Lau VWC, Huang Z, Hamidzhadeh K, Caplazi P, et al. The kinase TPL2 activates ERK and p38 signaling to promote neutrophilic inflammation. *Sci Signal.* 2017; 10:eaah4273. [PubMed: 28420753]
- Rousseau S, Papoutsopoulou M, Symons A, Cook D, Lucocq JM, Prescott AR, O'Garra A, Ley SC, Cohen P. TPL2-mediated activation of ERK1 and ERK2 regulates the processing of pre-TNF alpha in LPS-stimulated macrophages. *J Cell Sci.* 2008; 121:149–154. [PubMed: 18187448]
- McNab FW, Ewbank J, Rajsbaum R, Stavropoulos E, Martirosyan A, Redford PS, Wu X, Graham CM, Saraiva M, Tschlis P, et al. TPL-2-ERK1/2 signaling promotes host resistance against intracellular bacterial infection by negative regulation of type I IFN production. *J Immunol.* 2013; 191:1732–1743. [PubMed: 23842752]
- Kontoyiannis D, Boulougouris G, Manoloukos M, Armaka M, Apostolaki M, Pizarro T, Kotlyarov A, Forster I, Flavell R, Gaestel M, et al. Genetic dissection of the cellular pathways and signaling mechanisms in modeled tumor necrosis factor-induced Crohn's-like inflammatory bowel disease. *J Exp Med.* 2002; 196:1563–1574. [PubMed: 12486099]
- Jostins L, Ripke S, Weersma RK, Duerr RH, McGovern DP, Hui KY, Lee JC, Schumm LP, Sharma Y, Anderson CA, et al. International IBD Genetics Consortium (IIBDGC). Host-microbe interactions have shaped the genetic architecture of inflammatory bowel disease. *Nature.* 2012; 491:119–124. [PubMed: 23128233]

13. Hedl M, Abraham C. A *TPL2 (MAP3K8)* disease-risk polymorphism increases TPL2 expression thereby leading to increased pattern recognition receptor-initiated caspase-1 and caspase-8 activation, signalling and cytokine secretion. *Gut*. 2016; 65:1799–1811. [PubMed: 26215868]
14. Roulis M, Nikolaou C, Kotsaki E, Kaffe E, Karagianni N, Koliarakis V, Salpea K, Ragoussis J, Aidinis V, Martini E, et al. Intestinal myofibroblast-specific Tpl2-Cox-2-PGE2 pathway links innate sensing to epithelial homeostasis. *Proc Natl Acad Sci USA*. 2014; 111:E4658–E4667. [PubMed: 25316791]
15. Waterfield MR, Zhang M, Norman LP, Sun SC. NF-kappaB1/p105 regulates lipopolysaccharide-stimulated MAP kinase signaling by governing the stability and function of the Tpl2 kinase. *Mol Cell*. 2003; 11:685–694. [PubMed: 12667451]
16. Beinke S, Deka J, Lang V, Belich MP, Walker PA, Howell S, Smerdon SJ, Gamblin SJ, Ley SC. NF-kappaB1 p105 negatively regulates TPL-2 MEK kinase activity. *Mol Cell Biol*. 2003; 23:4739–4752. [PubMed: 12832462]
17. Papoutsopoulou S, Symons A, Tharmalingam T, Belich MP, Kaiser F, Kioussis D, O'Garra A, Tybulewicz V, Ley SC. ABIN-2 is required for optimal activation of Erk MAP kinase in innate immune responses. *Nat Immunol*. 2006; 7:606–615. [PubMed: 16633345]
18. Sriskantharajah S, Gückel E, Tsakiri N, Kierdorf K, Brender C, Ben-Addi A, Veldhoen M, Tschlis PN, Stockinger B, O'Garra A, et al. Regulation of experimental autoimmune encephalomyelitis by TPL-2 kinase. *J Immunol*. 2014; 192:3518–3529. [PubMed: 24639351]
19. Robinson MJ, Beinke S, Kouroumalis A, Tschlis PN, Ley SC. Phosphorylation of TPL-2 on serine 400 is essential for lipopolysaccharide activation of extracellular signal-regulated kinase in macrophages. *Mol Cell Biol*. 2007; 27:7355–7364. [PubMed: 17709378]
20. Windheim M, Stafford M, Peggie M, Cohen P. Interleukin-1 (IL-1) induces the Lys63-linked polyubiquitination of IL-1 receptor-associated kinase 1 to facilitate NEMO binding and the activation of IkappaBalpha kinase. *Mol Cell Biol*. 2008; 28:1783–1791. [PubMed: 18180283]
21. Pauls E, Nanda SK, Smith H, Toth R, Arthur JSC, Cohen P. Two phases of inflammatory mediator production defined by the study of IRAK2 and IRAK1 knock-in mice. *J Immunol*. 2013; 191:2717–2730. [PubMed: 23918981]
22. Gleason CE, Ordureau A, Gourlay R, Arthur JS, Cohen P. Polyubiquitin binding to optineurin is required for optimal activation of TANK-binding kinase 1 and production of interferon β . *J Biol Chem*. 2011; 286:35663–35674. [PubMed: 21862579]
23. Wiggin GR, Soloaga A, Foster JM, Murray-Tait V, Cohen P, Arthur JS. MSK1 and MSK2 are required for the mitogen- and stress-induced phosphorylation of CREB and ATF1 in fibroblasts. *Mol Cell Biol*. 2002; 22:2871–2881. [PubMed: 11909979]
24. Nanda SK, Venigalla RK, Ordureau A, Patterson-Kane JC, Powell DW, Toth R, Arthur JS, Cohen P. Polyubiquitin binding to ABIN1 is required to prevent autoimmunity. *J Exp Med*. 2011; 208:1215–1228. [PubMed: 21606507]
25. Wagner S, Carpentier I, Rogov V, Kreike M, Ikeda F, Löhr F, Wu CJ, Ashwell JD, Dötsch V, Dikic I, Beyaert R. Ubiquitin binding mediates the NF-kappaB inhibitory potential of ABIN proteins. *Oncogene*. 2008; 27:3739–3745. [PubMed: 18212736]
26. Emmerich CH, Ordureau A, Strickson S, Arthur JS, Pedrioli PG, Komander D, Cohen P. Activation of the canonical IKK complex by K63/M1-linked hybrid ubiquitin chains. *Proc Natl Acad Sci USA*. 2013; 110:15247–15252. [PubMed: 23986494]
27. Komander D, Reyes-Turcu F, Licchesi JD, Odenwaelder P, Wilkinson KD, Barford D. Molecular discrimination of structurally equivalent Lys 63-linked and linear polyubiquitin chains. *EMBO Rep*. 2009; 10:466–473. [PubMed: 19373254]
28. Rahighi S, Ikeda F, Kawasaki M, Akutsu M, Suzuki N, Kato R, Kensche T, Uejima T, Bloor S, Komander D, et al. Specific recognition of linear ubiquitin chains by NEMO is important for NF-kappaB activation. *Cell*. 2009; 136:1098–1109. [PubMed: 19303852]
29. Hu Y, Green N, Gavrin LK, Janz K, Kaila N, Li HQ, Thomason JR, Cuzzo JW, Hall JP, Hsu S, et al. Inhibition of Tpl2 kinase and TNFalpha production with quinoline-3-carbonitriles for the treatment of rheumatoid arthritis. *Bioorg Med Chem Lett*. 2006; 16:6067–6072. [PubMed: 16973359]

30. Kitajima S, Takuma S, Morimoto M. Changes in colonic mucosal permeability in mouse colitis induced with dextran sulfate sodium. *Exp Anim.* 1999; 48:137–143. [PubMed: 10480018]
31. Rakoff-Nahoum S, Paglino J, Eslami-Varzaneh F, Edberg S, Medzhitov R. Recognition of commensal microflora by toll-like receptors is required for intestinal homeostasis. *Cell.* 2004; 118:229–241. [PubMed: 15260992]
32. Okayasu I, Hatakeyama S, Yamada M, Ohkusa T, Inagaki Y, Nakaya R. A novel method in the induction of reliable experimental acute and chronic ulcerative colitis in mice. *Gastroenterology.* 1990; 98:694–702. [PubMed: 1688816]
33. Eliopoulos AG, Dumitru CD, Wang CC, Cho J, Tschlis PN. Induction of COX-2 by LPS in macrophages is regulated by Tpl2-dependent CREB activation signals. *EMBO J.* 2002; 21:4831–4840. [PubMed: 12234923]
34. Liu WK, Chien CY, Chou CK, Su JY. An LKB1-interacting protein negatively regulates TNF α -induced NF-kappaB activation. *J Biomed Sci.* 2003; 10:242–252. [PubMed: 12595760]
35. Leotoing L, Chereau F, Baron S, Hube F, Valencia HJ, Bordereaux D, Demmers JA, Strouboulis J, Baud V. A20-binding inhibitor of nuclear factor-kappaB (NF-kappaB)-2 (ABIN-2) is an activator of inhibitor of NF-kappaB (IkappaB) kinase alpha (IKKalpha)-mediated NF-kappaB transcriptional activity. *J Biol Chem.* 2011; 286:32277–32288. [PubMed: 21784860]
36. Hughes DP, Marron MB, Brindle NP. The antiinflammatory endothelial tyrosine kinase Tie2 interacts with a novel nuclear factor-kappaB inhibitor ABIN-2. *Circ Res.* 2003; 92:630–636. [PubMed: 12609966]

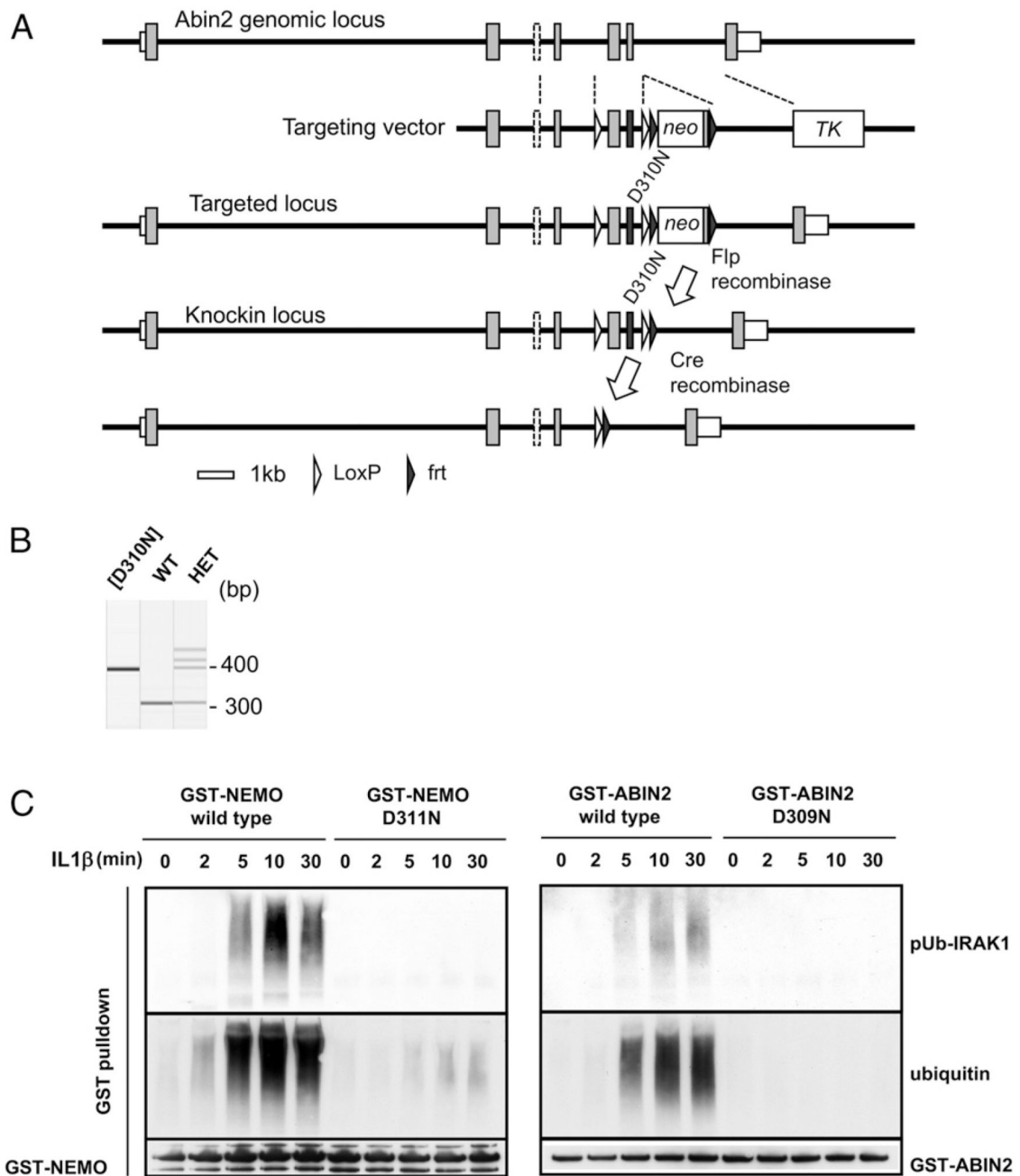


Figure 1.

Generation of ubiquitin-binding-defective ABIN2[D310N] knock-in mice. (A) A targeting vector was made to introduce the desired Asp310Asn mutation in exon 5 of the mouse *ABIN2* gene. In addition, LoxP sequences were introduced upstream of exon 4 and downstream of exon 6. The neomycin-selectable marker was flanked with Frt sites to allow its removal via the expression of Flp recombinase. This vector was used to generate targeted embryonic stem cells by conventional methods, which were then used to generate chimeric mice. Germline-transmitting chimeric mice were crossed to Flp transgenic mice to remove

the neomycin cassette. Subsequently, the allele was converted to a KO allele by crossing to mice expressing a Cre transgene. (B) The primers generate a 350-bp PCR product for the wild-type (WT) allele and 400-bp product for the ABIN2[D310N] knock-in allele (or 500-bp product for a knock-in allele before excision of the neomycin cassette). (C) IL-1R cells transfected with constructs encoding either WT human GST-NEMO, human GST-NEMO[D311N], human WT GST-ABIN2, or human GST-ABIN2[D309N] were stimulated with IL-1 β for the times indicated. After 24 h, the cells were starved for 16 h, stimulated with 5 ng/ml IL-1 β for times indicated, and then cells were lysed with buffer (50 mM Tris-HCl [pH 7.5], 1 mM EGTA, 1 mM EDTA, 1% [wt/vol] Triton X-100, 1 mM Na₃VO₄, 50 mM NaF, 5 mM sodium pyrophosphate, 10 mM sodium glycerophosphate, 0.27 M sucrose, 50 mM iodoacetamide, 1 mM benzamide, 0.2 mM PMSF), and cell extracts were prepared. To precipitate proteins bound to GST-ABIN2, an aliquot of cell extract (0.5 mg protein) was added to 20 μ l of glutathione-Sepharose beads and after 1 h of incubation at 4°C the beads were collected by centrifugation and washed three times with 1 ml lysis buffer and once with 1 ml 10 mM Tris-HCl (pH 8). The bound proteins were released by denaturation in 1% SDS, separated on SDS-PAGE, and transferred to PVDF membranes; immunoblotting was carried out with anti-IL receptor-associated kinase 1 (IRAK1) (top panels) and anti-ubiquitin. NEMO, NF- κ B essential modulator. The anti-IRAK1 and anti-ubiquitin Abs were obtained from Santa Cruz Biotechnology.

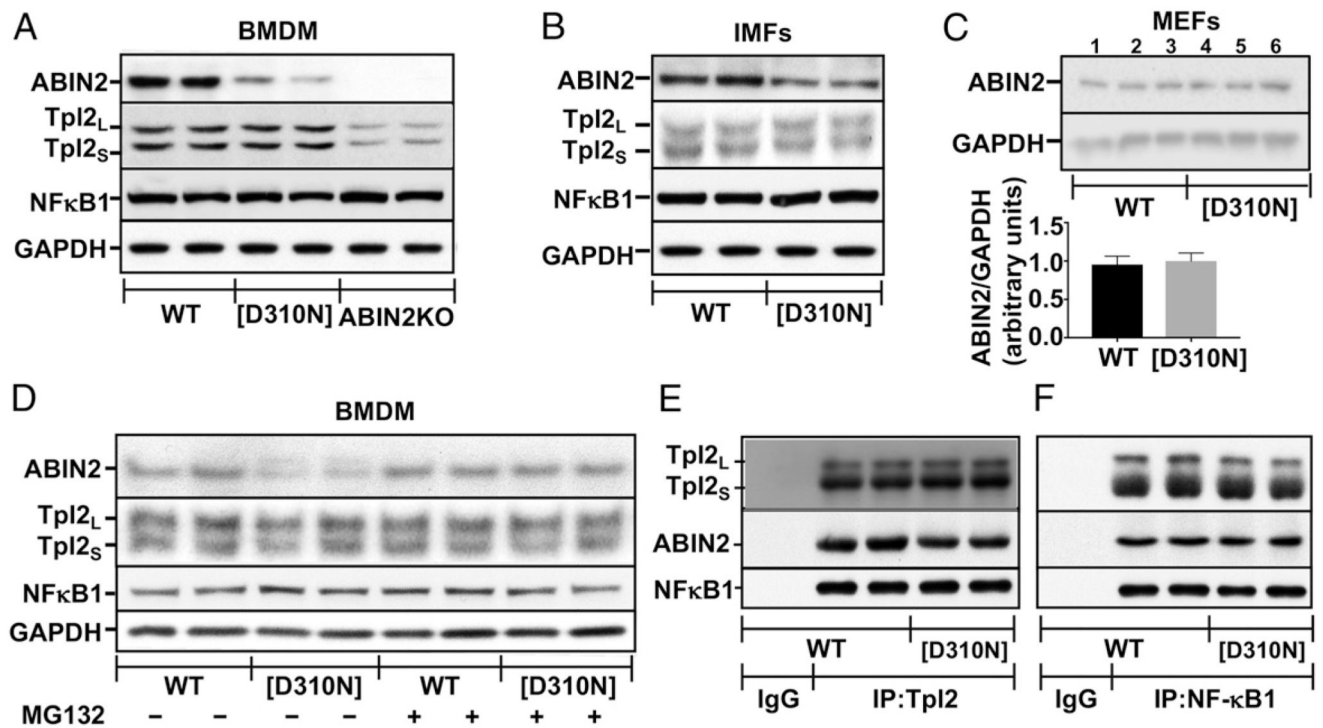


Figure 2.

Expression of ABIN2 and Tpl2 in cells from ABIN2[D310N] and KO mice. **(A)** BMDM extracts (20 μg protein) from WT mice, ABIN2 [D310N] knock-in, and ABIN2 KO mice were subjected to SDS-PAGE and immunoblotted with Abs recognizing ABIN2, Tpl2, and NF-κB1. Abs to GAPDH were used as a loading control. **(B)** As in (A), except that IMF from WT and ABIN2[D310N] mice were used. **(C)** Same as (A), except that MEFs from three different WT embryos (1–3) and three different ABIN2[D310N] embryos (4–6) were used. **(D)** Same as (A), except that BMDM from WT and ABIN2[D310N] mice were incubated for 4 h with or without 5 μM MG132 prior to cell lysis. **(E)** Tpl2 was immunoprecipitated (IP) from BMDM extracts of WT or ABIN2[D310N] mice using anti-Tpl2 or control IgG. The IPs were performed in duplicate. The IPs were washed, dissolved in SDS, subjected to SDS-PAGE, and immunoblotted with Abs recognizing Tpl2, ABIN2, and NF-κB1. **(F)** As in (E), except that NF-κB1 was immunoprecipitated instead of Tpl2. (A–F) Similar results were obtained in at least two independent experiments.

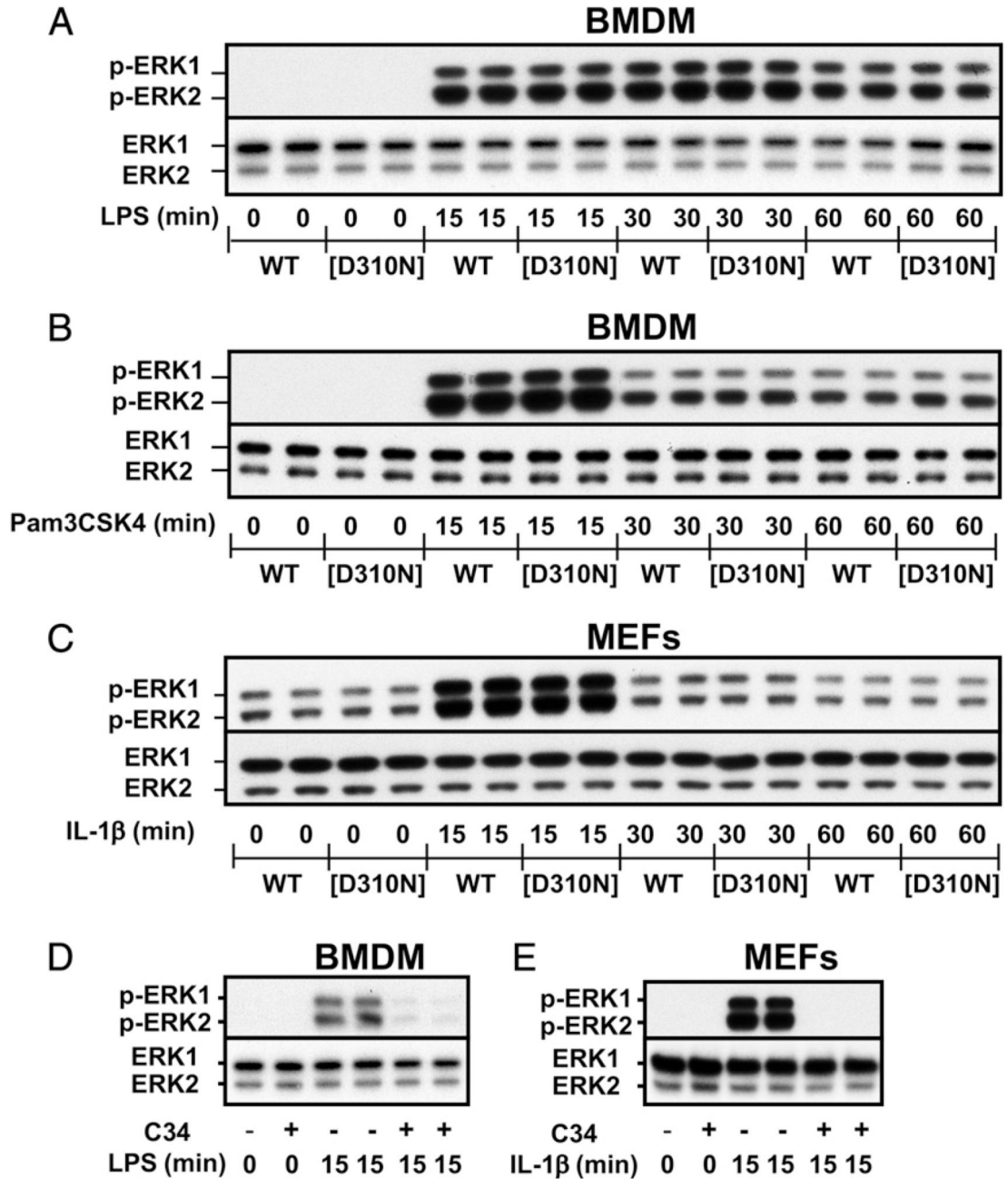
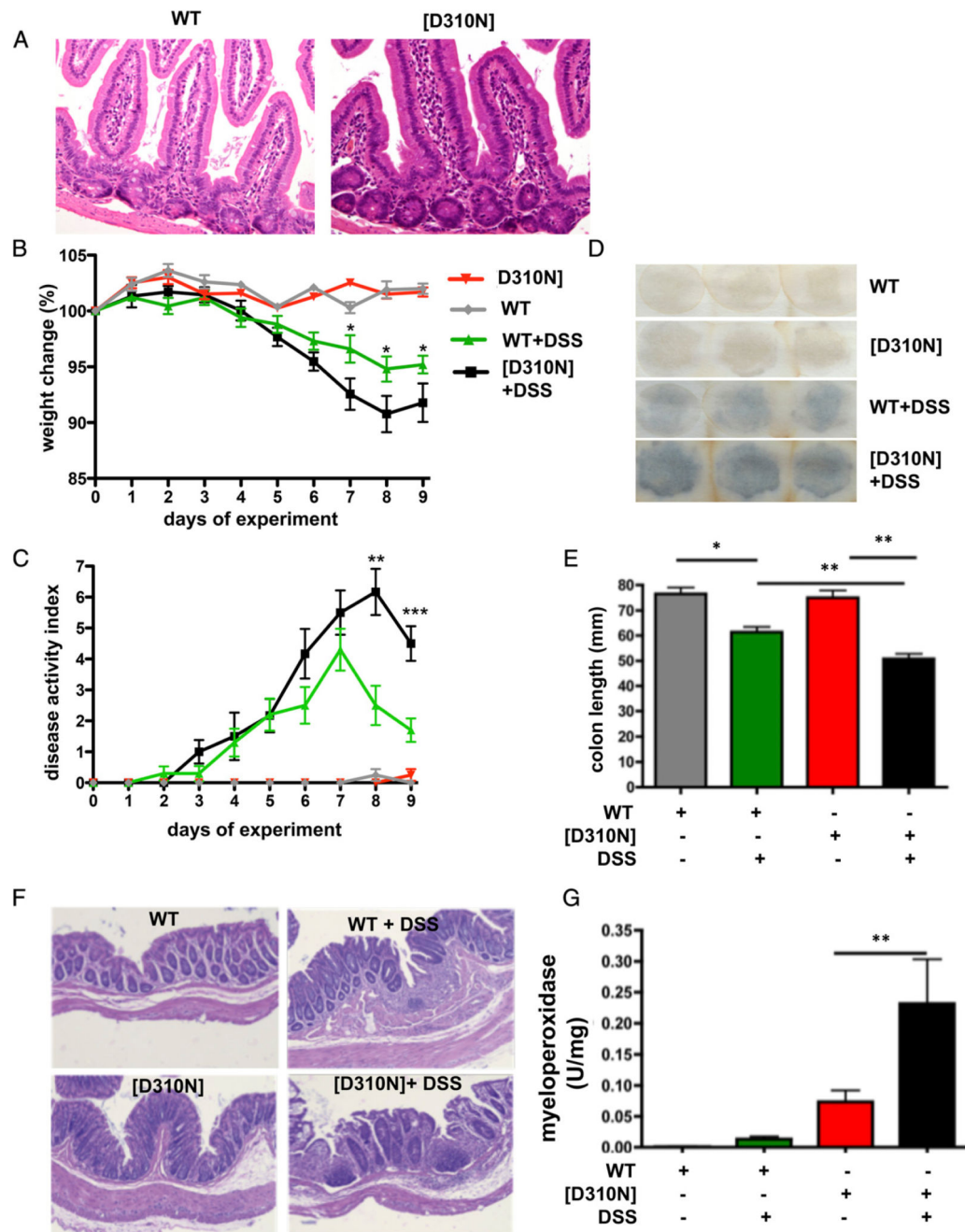


Figure 3. The Tpl2-dependent activation of ERK1 and ERK2 in BMDM and MEFs from ABIN2[D310N] mice is similar to WT mice. (A) BMDM from WT and ABIN2[D310N] mice were stimulated with 10 ng/ml LPS for the times indicated, and cell extract (20 μg protein) was subjected to SDS-PAGE and immunoblotting with Abs recognizing ERK1/ERK2 phosphorylated at their Thr-Glu-Tyr motifs (p-ERK1, p-ERK2) and all forms of ERK1 and ERK2. (B) As in (A), except that the cells were stimulated with Pam3CSK4 (1.0 μg/ml). (C) As in (A) and (B), except that MEFs were stimulated with 5 ng/ml mouse IL-1β.

(D) BMDM from WT mice were incubated for 1 h without (–) or with (+) 3 μ M of the Tpl2 inhibitor C34, then stimulated with 10 ng/ml LPS for the times indicated. Cells were lysed, subjected to SDS-PAGE, and immunoblotted with the Abs in (A). **(E)** As in (D), except that MEFs were stimulated with IL-1 β . (A–E) Similar results were obtained in at least three independent experiments.

**Figure 4.**

ABIN2[D310N] mice display an intestinal phenotype and are hypersensitive to DSS-induced colitis. (A) Representative photomicrograph showing an H&E-stained section of the small intestine from WT ($n = 4$) and ABIN2[D310N] ($n = 5$) mice. (B–E) WT ($n = 12$) and ABIN2[D310N] ($n = 12$) mice were fed 2.5% DSS solution in drinking water for 5 d followed by regular drinking water for 4 d. Mice were sacrificed on ninth day after DSS was first administered to measure colon length and to perform histopathology. (B) Percentage change in body weight compared with body weight at the start of the experiment. (C) DAI.

(D) Representative image of four mice per group showing rectal bleeding (blue) in fecal pellets on day 6. (E) Colon lengths (millimeters) of untreated and DSS-treated groups. (F) Representative photomicrograph showing histopathological changes in the colon tissue as examined by H&E staining. Original magnification $\times 20$ (A), $\times 2$ (D), and $\times 10$ (F). (G) Myeloperoxidase enzymatic activity of colonic tissue from ABIN2[D310N] and WT mice before and after treatment with DSS. Data are the mean and SEM from 4 to 12 mice per group and are representative of two separate experiments. Student *t* test was used to test for statistical differences between DSS-treated groups. * $p < 0.05$, ** $p < 0.01$, *** $p < 0.001$.

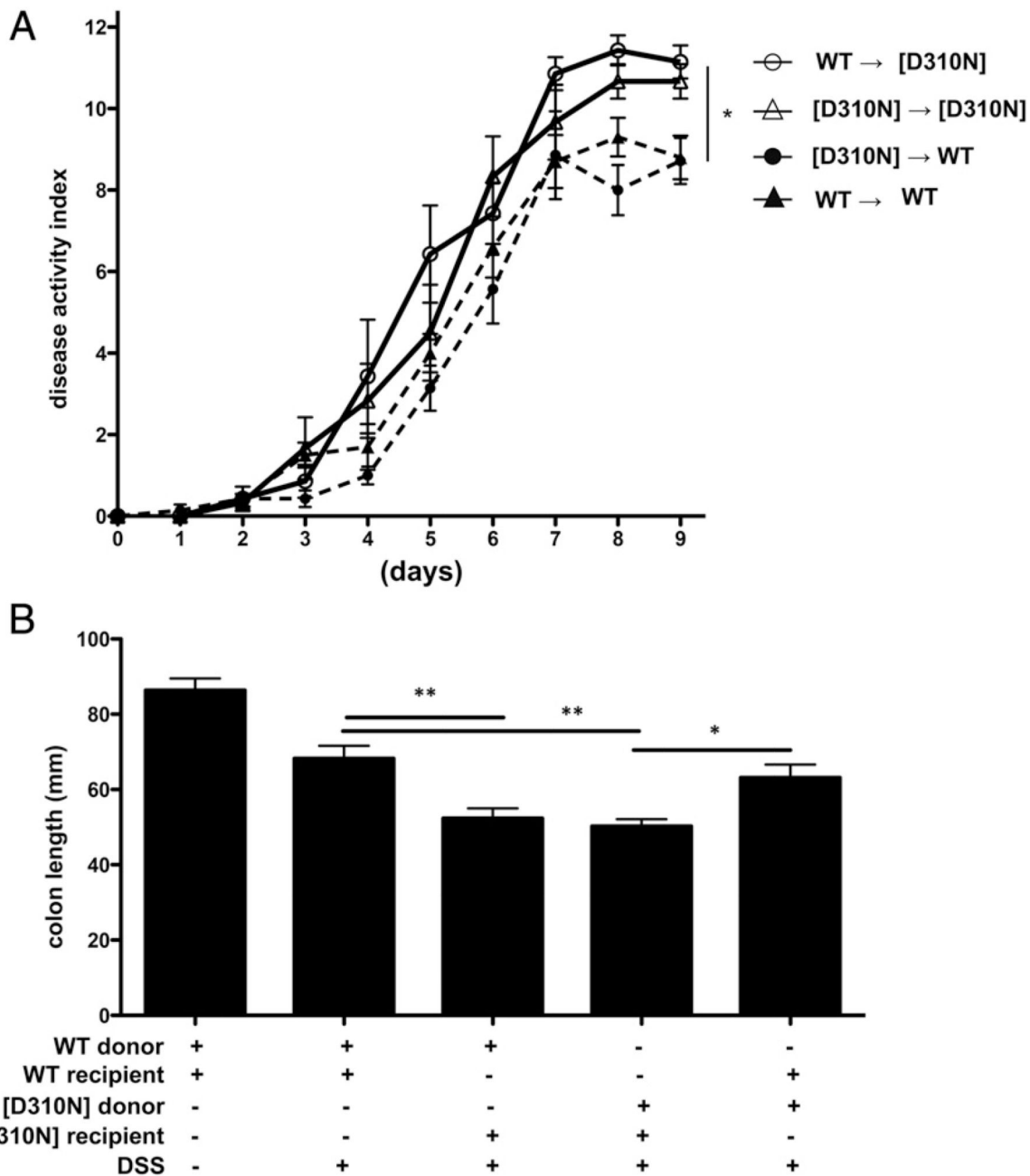


Figure 5. Bone marrow chimera showing the cell type responsible for driving the colitis phenotype in the ABIN2[D310N] mice. Bone marrow chimeras were constructed by injecting donor bone marrow cells through the tail vein of lethally irradiated recipient mice. After 6 wk, chimeric mice ($n = 5-10$ mice per group) were treated for 5 d with 2.5% (w/v) DSS, followed by regular drinking water for 4 d. Mice were sacrificed on the ninth day after DSS was first administered to measure colon length. (A) Graph showing the DAI. Statistical analysis was performed by ANOVA and Tukey multiple comparison test of group area under curve data

from 5 to 10 individual mice per group. **(B)** Graph showing the length of colon (millimeters). (A and B) Data are the mean and SEM from 5 to 10 mice per group and are representative of two separate experiments. Student *t* test was used to test for statistical differences between DSS-treated groups. **p* < 0.05, ***p* < 0.01.

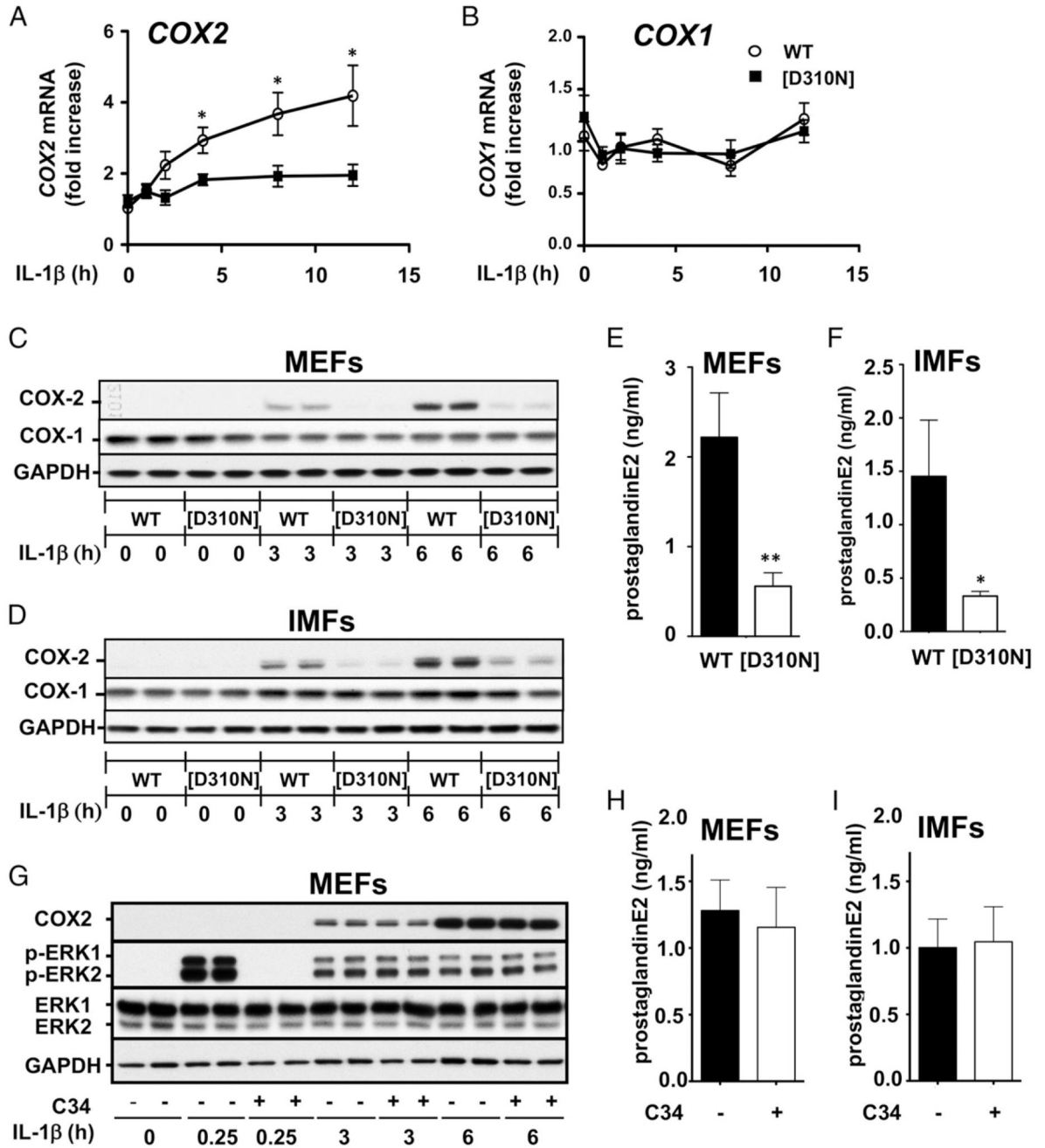


Figure 6.

The IL-1β-stimulated reduction of COX2 and PGE₂ in fibroblasts from ABIN2[D310N] mice is independent of Tpl2 activity. (A and B) MEFs from WT (open circles) or ABIN2[D310N] (closed squares) mice were stimulated with IL-1β for the times indicated, and the expression of *COX2* mRNA (A) or *COX1* mRNA (B) was quantitated by quantitative RT-PCR. (A and B) Data are the mean and SEM with MEFs from five to six embryos per group and are representative of two separate experiments. Mann-Whitney *U* test was used to test for statistical differences. **p* < 0.05. (C) MEFs or (D) IMFs from WT or

ABIN2[D310N] mice were stimulated with IL-1 β for the times indicated. Cells were lysed, subjected to SDS-PAGE, and then immunoblotted with Abs recognizing COX2, COX1, and GAPDH. (C and D) Similar results were obtained in at least two independent experiments. (E and F) The secretion of PGE₂ from MEFs (E) and IMFs (F) was quantitated by ELISA 6 h after stimulation with IL-1 β . (G) MEFs from WT mice were incubated for 1 h without or with 3 μ M of the Tpl2 inhibitor C34, then stimulated with 5 ng/ml of IL-1 β for the times indicated. Cells were lysed, subjected to SDS-PAGE, and immunoblotted with the Abs in Fig. 3 and with GAPDH as a loading control. Similar results were obtained in two independent experiments. (H and I) Same as (G), secretion of PGE₂ from MEFs (E) and IMFs (F) was quantitated by ELISA 6 h after stimulation with IL-1 β . (E, F, H, and I) Data are the mean and SEM with cells from five to six embryos or pups per group and are representative of two separate experiments. Mann-Whitney *U* test was used to test for statistical differences. **p* < 0.05, ***p* < 0.01.